Emergent Electromagnetic Induction and Adiabatic Charge Pumping in Noncentrosymmetric Weyl Semimetals

Hiroaki Ishizuka,[1] Tomoya Hayata,[2] Masahito Ueda,[3,4] and Naoto Nagaosa[1,4]
[1]Department of Applied Physics, The University of Tokyo, Bunkyo, Tokyo 113-8656, Japan
[2]Department of Physics, Chuo University, 1-13-27 Kasuga, Bunkyo, Tokyo 112-8551, Japan
[3]Department of Physics, The University of Tokyo, 7-3-1 Hongo, Bunkyo, Tokyo 113-8656, Japan
[4]RIKEN Center for Emergent Matter Science (CEMS), Wako, Saitama 351-0198, Japan
(Received 21 July 2016; revised manuscript received 25 September 2016; published 18 November 2016)

The photovoltaic effect due to the adiabatic quantum phase in noncentrosymmetric Weyl semimetals is studied. We particularly focus on the case in which an external ac electric field is applied. By considering a generalized Weyl Hamiltonian with nonlinear terms, we show that the photocurrent is induced by circularly, rather than linearly, polarized light. This photovoltaic current can be understood as an emergent electromagnetic induction in momentum space; the Weyl node is a magnetic monopole in momentum space, the circular motion of which induces the electric field. This result is distinct from conventional photovoltaic effects, and the estimated photocurrent is $\sim 10^{-1}$–10^{1} nA, which can be detected experimentally.

DOI: 10.1103/PhysRevLett.117.216601

Introduction.—The nontrivial phase in quantum adiabatic processes—Berry's phase—is one of the fundamental aspects of quantum mechanics. In a quantum system, the presence of an energy gap often prohibits excitations to higher-energy states, and confines electrons within a Hilbert subspace composed of lower energy states. In dynamical processes, the confinement sometimes gives rise to an additional geometric phase that depends only on the path, and not on the details of the dynamics.

Ever since its discovery [1], it has been revealed that Berry's phase leads to rich physics. Interestingly, such an effect appears not only in mesoscopic systems, but also in the macroscopic properties of bulk materials. In solid-state materials, Berry's phase of electrons leads to nontrivial properties of solids, such as fractional pseudorotation quantum numbers in Jahn-Teller systems [2–4] and topological Hall effects [5,6] arising from noncollinear magnetic textures. A similar nontrivial structure of wave functions shows up in the Brillouin zone, and contributes to nontrivial electronic states [7,8] and transport phenomena [9–11].

Berry's phase also affects the dynamics of nonequilibrium systems. In periodically driven systems, it is known that the adiabatic phase induces the quantized pumping of charge [12–14]. In an insulator, the pumping of charge is related to the time average of the emergent electric field defined by [12]

$$e_n^a(\vec{k}) = \partial_t A_n^a(\vec{k}) - \partial_a A_n^t(\vec{k}), \tag{1}$$

where

$$A_n^a(\vec{k}) = -i\langle u_{n\vec{k}}(t)|\partial_a|u_{n\vec{k}}(t)\rangle \tag{2}$$

is Berry's connection in momentum space with $\partial_a \equiv \partial/\partial k_a$ $(a = x, y, z)$ and $\partial_t \equiv \partial/\partial t$. However, in solids, the contribution from such an effect is usually zero or vanishingly small, where the energy scale of the driving field is much smaller than that of the bandwidth.

In this Letter, we show that the effect of the $\vec{e}$ field on the charge pumping is enhanced in Weyl semimetals (WSMs), and possibly leads to experimentally observable consequences. Intuitively, this could be understood as an electromagnetic induction in momentum space. Suppose we have a Weyl node at a nonzero k_z and $k_x = k_y = 0$. In the situation, a coupling of electrons to external electric fields can induce a shift of the node in the k_x-k_y plane. In the case of circularly polarized light, the incident light results in a rotational motion of the Weyl node as schematically shown in Fig. 1(a). As the Weyl nodes can be seen as the "magnetic monopoles" of Berry's connection in momentum space, in analogy to the symmetric Maxwell's equation in real space, the circular motion of a Weyl node induces the dc $\vec{e}$ field penetrating through the orbit. Since the $\vec{e}$ field is related to the electric current as $\vec{j} \propto \vec{e}$ [12], the incident light can induce a dc current along the z axis.

As is shown later, the photocurrent arises only with the circularly polarized light, in contrast to the conventional anomalous photocurrents [15] and those induced through Berry's curvature [10,11]. Also, it does not require a change in the charge distribution; this is yet another feature distinct from the photocurrents induced through Berry's curvature and those in WSMs with broken time-reversal symmetry [16,17], in which a change in the charge distribution is necessary to induce a photocurrent. We note that our "intrinsic" photocurrent is sensitive to the direction of the incident light, in contrast to the other photocurrents in

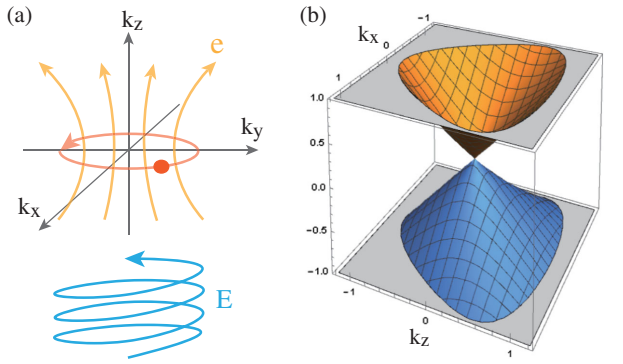

FIG. 1. (a) Schematic figure of the emergent electric field induced by incident light. The red dot indicates the position of a Weyl node in the presence of the incident light. The incident electric field induces a rotational motion of the Weyl node. The orbital motion of the Weyl node induces a dc emergent electric field penetrating through the orbit (yellow lines), which is, parallel to the propagation direction of the light. (b) Dispersion relations of the Weyl Hamiltonian with quadratic terms; $v = v_z = 1$, $\alpha_1 = 0$, and $\alpha_2 = -1$.

WSMs. Recently, possible realizations of the WSM in solids have been explored in various systems [18–34]. The phenomenon we propose here should give rise to an observable photocurrent in the WSM that lacks spatial-inversion symmetry, such as in TaAs [30–34].

Since the photocurrent induced by a change in the electron distribution has been well studied [10,11,16,17], in this Letter we focus on the contribution from the adiabatic quantum phase. In the following, we first elaborate on some general requirements for free fermion systems to have a net $\vec{e}$ field. Based on this picture, we discuss a potential enhancement of the $\vec{e}$ field in WSMs. For this purpose, in the latter half, we particularly consider a generalized Weyl Hamiltonian with nonlinear terms, which couples to an external electric field by a symmetry allowed coupling. In this model, we show that shining the circularly polarized light induces an electric current parallel to $\vec{k}^{(i)}$, the vector connecting the Γ point and the ith Weyl node.

$\vec{e}$ field in periodically driven systems.—In a periodically driven system, where the Hamiltonian $H(\{D_i\})$ is driven by slowly varying parameters $D_i = D_i(t) = D_i(t+T)$ $(i = 1, 2, \ldots, m)$, the average $\vec{e}$ field over a period reads

$$e_n^a(\vec{k}) = \partial_a \int_0^T [-A_n^t(\vec{k})]dt' \tag{3}$$

$$= \sum_{i\neq j} i\partial_a \int_S dD_i \wedge dD_j \partial_{D_j} \langle u_{n\vec{k}}(t)|\partial_{D_i}|u_{n\vec{k}}(t)\rangle, \tag{4}$$

where the region S indicates a surface enclosed by the path given by $\{D_i(t)\}$ $(0 \le t < T)$. This is an $m-1$ dimensional hypersurface, and the integral does not depend on the choice of the surface. The integral in Eq. (3) is Berry's phase in an adiabatic process [1]. From Eq. (4), if $m = 1$, there is no net $\vec{e}$ field in periodically driven systems since the area covered by the integral in Eq. (4) is zero.

For a fully filled electron band, the average $\vec{e}$ field over one period of the cycle is given by

$$e_n^a(\vec{k}) = -\partial_a \int_0^T A_n^t(\vec{k})dt', \tag{5}$$

and the sum over the Brillouin zone reads

$$\bar{e}_n^a = -\int \prod_{b\neq a} dk_b \int_0^T A_n^t(\vec{k})dt'\Big|_{-\pi}^{\pi}. \tag{6}$$

Here, we set the lattice constant to unity. It has been pointed out that, in insulators, the charge pumped during the adiabatic process is proportional to Eq. (6) [12], and that the integrand on the right-hand side of Eq. (6) gives a quantized value due to the single valuedness of the wave function.

In an insulator, however, it is expected that e^a induced by an electromagnetic field generally remains zero since the pumped current is a topologically protected quantity, and the external field is perturbatively small. In a two-band model, this can be seen from the fact that $\bar{e}^a$ is given by

$$\bar{e}_{\pm}^a = \mp \frac{1}{2}\int d^3k \int_0^T dt \hat{\vec{R}}(\vec{k},t)\cdot\partial_a\hat{\vec{R}}(\vec{k},t)\times\partial_t\hat{\vec{R}}(\vec{k},t). \tag{7}$$

Here, $n = +$ $(-)$ denotes the conduction (valence) band, $\hat{\vec{R}}(\vec{k},t)$ is the normalized vector of $R_\nu(\vec{k},t)$ $(\nu = x, y, z)$, and $\hat{R}_\nu(\vec{k},t) = R_\nu(\vec{k},t)/R$ with $R = |\vec{R}(\vec{k},t)|$. The Hamiltonian is given by

$$H(\vec{k},t) = \sum_\nu \sigma_\nu R_\nu(\vec{k},t), \tag{8}$$

where σ_ν $(\nu = x, y, z)$ are Pauli matrices. The right-hand side of Eq. (7) gives the number of times $\hat{\vec{R}}$ wraps a unit sphere upon mapping $(k_\mu, t) \to S^2$ by $\vec{R}(\vec{k},t)$. In an insulator, since the energy scale of an external field is typically much smaller than that of the electron bandwidth, we naturally expect that this wrapping number becomes zero.

In a doped case, the contribution from doped carriers gives a nonzero e_n^a. In a slightly doped insulator, however, the contribution remains very small since the surface of the sphere covered in Eq. (7) remains very small.

Nonlinear Weyl Hamiltonian.—An exception to such cases, in which charge doping leads to a large e_n^a field, is a WSM. In a WSM, the effective Hamiltonian at the node is given by $H = 0$. Hence, the Hamiltonian close to the node is dominated by external fields. As a consequence, a large e_n^a field is expected by doping carriers to the node. To study the $\vec{e}$ field in periodically driven systems, we consider a doped Weyl Hamiltonian with nonlinear terms and multiple external fields, whose Hamiltonian is given by Eq. (8) with

$$R_x(\vec{k}) = vk_x + gD_y + \frac{\alpha_2}{2}k_xk_z, \tag{9a}$$

$$R_y(\vec{k}) = vk_y - gD_x + \frac{\alpha_2}{2}k_yk_z, \tag{9b}$$

$$R_z(\vec{k}) = v_zk_z + \frac{\alpha_1}{2}(k_x^2 + k_y^2 - 2k_z^2), \tag{9c}$$

where the k_a's are wave numbers at the Weyl node. We here assume that the z-axis connects two Weyl nodes related by time-reversal or spatial-inversion symmetry operation; i.e., $\vec{k}^{(i)}$ is parallel to the z axis. In Eq. (9), the second terms in $R_x(\vec{k})$ and $R_y(\vec{k})$ are the couplings with the electric field of frequency ω and phase shift χ:

$$D_x = D\cos(\omega t), \tag{10}$$

$$D_y = D\sin(\omega t + \chi). \tag{11}$$

The electric field is circularly polarized for $\chi = 0$ and π, while it is linearly polarized for $\chi = \pi/2$ and $3\pi/2$. These couplings are allowed in general, if Weyl nodes are located away from symmetric points. When Weyl nodes are close to the Γ points, these terms appear from a coupling like

$$H_{el} = \tilde{g}\epsilon_{abc}D_a\kappa_b\hat{O}_c, \tag{12}$$

where κ_b is the wave number from the Γ point, $\hat{O}_\alpha$ ($\alpha = x$, y, z) is a set of operators that transform as vectors, and ϵ_{abc} is the Levi-Civita symbol. The third [second] terms in $R_x(\vec{k})$ and $R_y(\vec{k})$ [$R_z(\vec{k})$] are quadratic in k_a. These terms break the C_2 rotation about an axis in the xy plane; i.e., $+k_z$ and $-k_z$ become asymmetric as shown in Fig. 1(b). These terms reflect the existence of the pair node. Since our Hamiltonian includes the information about the presence of the pair node, which always exists in a material, we believe that our Hamiltonian in Eq. (9) is a generic model for Weyl semimetals in solids.

We first consider the case of electron doping. To evaluate the $\vec{e}$ field, we focus on the limit $\alpha_i \ll v/|\mu|$, $v_z/|\mu|$, where μ is the chemical potential ($\mu > 0$ and $\mu < 0$ for electron and hole doping, respectively). To calculate $\bar{e}^a$, we expand the $\vec{e}$ field up to second order in α_i.

In the adiabatic regime, the electron filling is not changed by applying electric fields; the electron distribution is fixed to the case of $D_x = D_y = 0$. To take into account the change of the Fermi surface by α_i, we expand the dispersion relation around the Fermi surface for $\alpha_{1,2} = 0$ along the radial direction. For the electron doped case, the change in k_F, Δk, can be calculated by solving

$$\mu - \varepsilon(\vec{k}_F^{(0)}) + \Delta k\partial_k\varepsilon(\vec{k}_F^{(0)}) = 0, \tag{13}$$

where $\vec{k}_F^{(0)}$ is the Fermi surface for $\alpha_{1,2} = 0$. From the fact that $\mu - \varepsilon(\vec{k}_F) \sim O(\alpha_i)$, we expect $\Delta k \sim O(\alpha_i)$. Hence, in general, we need to consider terms up to $O(\Delta k^2)$ to fully take into account terms up to $O(\alpha_i^2)$. However, from explicit calculation, we find that the $O(\alpha_i^2)$ contribution to Δk vanishes.

Within this approximation, we obtain the analytic form of $\bar{e}^z$ for v, $v_z \gg \alpha_i k_F$. The second-order response in D, up to $O(\alpha_i^2)$, gives a net emergent electric field for the node, along the z axis:

$$\bar{e}^z_{R,L} = \bar{e}^z_{+R,L} = \pm\pi\frac{4(v^2 - 2v_z^2)\alpha_1 - 3vv_z\alpha_2}{30v^5v_z^3} \times \alpha_1(\mu g D)^2\omega\cos(\chi). \tag{14}$$

Here, the $+$ and $-$ signs are for Weyl (R) and anti-Weyl nodes (L), respectively. Because of the phase factor $\cos(\chi)$, the $\vec{e}$ field shows a maximum for the circular light ($\chi = 0$, π), while it vanishes for the linearly polarized light ($\chi = \pi/2$, $3\pi/2$). This is consistent with the general argument above, and indicates the absence of a dc $\vec{e}$ field when we have only one time-dependent parameter.

For electron doping, the net emergent electric field increases as a function of μ^2. This indicates that the contribution from electrons with energy ε decays like $\vec{e} \sim \varepsilon^{-1}$, as the density of states is approximately proportional to ε^2. Therefore, when considering hole doping, we need to appropriately take into account the contribution from electron states in the UV limits. However, from the argument above, $\bar{e}$ naturally vanishes for the filled bands. Therefore, we can evaluate the $\vec{e}$ field for the hole doped case by subtracting the contribution from vacant states. For the model in Eq. (9), the resultant $\bar{e}^z_{R,L}$ becomes the same with Eq. (14).

Finally, to give an estimate for the magnitude of the current, we here estimate the coupling g from the coupling of electron Wannier orbitals to the electric polarization operator. Considering that the polarization is given by $\sim q_e\langle|\delta r|\rangle$, where q_e is the elementary charge and δr is the distance from the center from the Wannier orbital, we estimate the coupling term to be of order $g \sim 10^{-29}$ J m/V [35]. Assuming $v \sim v_z \sim 10^{-29}$ Jm (this corresponds to the Fermi velocity of $\sim 10^5$ m/s), $\alpha_{1,2} \sim 10^{-39}$ J m^2, $\omega \sim 10^{13}$ Hz, the electric permittivity $\varepsilon \sim 10^{-10}$ F/m, and the light power of the incident light $\sim 10^5$ W/m^2, the estimated strength of the current is about 10^{-1}–10^1 nA in a 1 mm^3 sample [36].

Models with multiple Weyl nodes.—In the WSM, there always exist multiple Weyl nodes [37]. Applications of our theory to multiple nodes are straightforward; the photocurrent is given by the sum of the contribution from each node.

From the symmetry point of view, in solids, the presence of Weyl nodes requires the breaking of either time-reversal or spatial-inversion symmetry. In the case of WSMs with broken time-reversal symmetry, and in the presence of spatial-inversion symmetry, a Weyl node has an equivalent companion anti-Weyl node. Since these two nodes are related by spatial-inversion symmetry, when a Weyl node is doped, there always exists an anti-Weyl node with exactly the same doping. For the photocurrent, since the sign of the induced current depends on the chirality, the effect of an electric field always cancels out and the total $\vec{e}$ field (electric current) vanishes. This is consistent with the general argument that the photovoltaic effect in $O(E^2)$ requires the breaking of spatial-inversion symmetry.

In contrast, in the case of WSMs with broken spatial-inversion symmetry, a Weyl (anti-Weyl) node has a companion Weyl (anti-Weyl) node. Hence, there always exist at least four nodes in the Brillouin zone (see Fig. 2) [38]. In such models, the parameters in the Hamiltonian in Eq. (9) are generally different between different pairs of Weyl nodes. The doping level (μ) also differs for each pair. Therefore, the emergent electric fields from Weyl and anti-Weyl pairs have different values; the net $\vec{e}$ field becomes nonzero. Therefore, the current induced by the emergent electromagnetic induction should be observed in the WSM with broken spatial-inversion symmetry.

Discussions.—In the mechanism presented here, the coupling of the external electric field to the electron orbitals, e.g., the coupling we considered, plays an important role. This is due to the fact that Berry's phase arises from the nontrivial change of the Bloch wave function over the period of the cycle. It gives rise to a different consequence from the Peierls substitution terms, whose nonlinear responses have been studied recently [16,17,39].

In our result, the photocurrent is induced by the adiabatic dynamics of electron orbitals; a change in the electron distribution is not required. Also, since the current is proportional to Berry's phase, the photocurrent arises only for the circularly polarized light while no current arises for the linearly polarized light. Another important feature of the coupling to electron orbitals is its anisotropy. Since Weyl nodes in solids are generally located away from symmetric points in the Brillouin zone, the coupling to electron orbitals is generally anisotropic. For instance, in the case of the coupling given by Eq. (14), in the lowest-order approximation, the coupling exists only for the x and y directions as in the Hamiltonian in Eq. (9). As a consequence, the photocurrent is expected to be highly sensitive to the direction of the incident light.

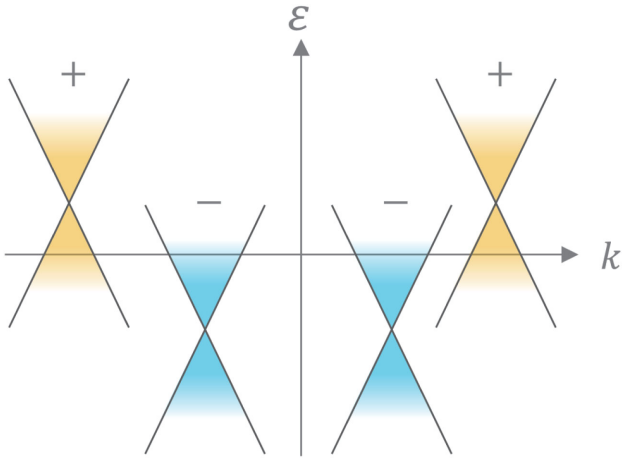

FIG. 2. Schematic picture of a Weyl semimetal with broken spatial-inversion symmetry. Each cone indicates a Weyl node and the sign shows the chirality. In the presence of time-reversal symmetry, two Weyl nodes with the same chirality are related by this symmetry operation, so that there are at least four Weyl nodes in the Brillouin zone.

In addition to the orbital coupling terms, the Peierls substitution terms can contribute to photocurrents in the WSM. Such photovoltaic effects in WSMs have been theoretically studied in the case of broken time-reversal symmetry [16,17]. In these theories, however, the change in the electron distribution, either by the chiral magnetic effect [16] or by the transfer of the photon angular momentum to electrons [17] plays a key role in the photovoltaic effect. In contrast, the mechanism studied in this Letter does not involve a change in the electron distribution.

In experiments, both mechanisms contribute to the photocurrent in WSMs. Naively, the contribution from the change in the distribution, i.e., the contribution from the Peierls substitution terms, becomes more important as the absorption of photons increases; the contribution is expected to be small if $\hbar\omega \ll \mu$. By considering $v \sim v_z \sim 10^{-29}$ J m and doping of electrons per node $x \sim 10^{-2}$, the condition gives $\omega \ll 10^{13}$——10^{15} Hz. Another criterion is given by the violation of the adiabatic approximation. This could be estimated from the condition that the amplitude of the wave function in the valence band becomes much smaller than that of the conduction band. We find that the criterion is $\omega \ll 10^{21}$——10^{23} Hz for the relaxation time $\tau \sim 10^{-12}$ s, $g \sim 10^{-29}$ J m/V, and the optical power 10^5 W/m^2.

Our mechanism can also be distinguished from the Peierls substitution mechanism because of its anisotropy. In our mechanism, as mentioned above, the photocurrent from each node is highly anisotropic. In materials, it is given by the sum of the contribution from all nodes, so that the anisotropy in the net photocurrent depends on the band structure. However, it can become highly anisotropic with a small uniaxial symmetry breaking. In contrast, the one by the Peierls substitution mechanism would be almost isotropic regardless of the band structure, since the Hamiltonian in the lowest-order approximation preserves the $SO(3)$ rotational symmetry under the Peierls substitution.

We also note that even in the WSM with broken time-reversal symmetry, it might be possible by the chiral magnetic effect [40–43] to make a difference in doping levels of Weyl–anti-Weyl pairs, and to break the cancellation of photocurrent between them. In this mechanism, the application of dc electric and magnetic fields induces chiral charge proportional to the inner product of the electric and magnetic fields. Hence, consideration of the chiral magnetic effect leads to a nonzero photocurrent. In this case, the photocurrent is observed as a correction to the conductivity, where its sign changes by changing the polarization from the right hand to the left.

Besides the WSM, the argument on the enhancement of the $\vec{e}$ field potentially applies to other nodal (semi)metals, such as the surface state of topological insulators, double Weyl [21,22,28,29] and Dirac [44,45] semimetals, as well

as those with quadratic band touching [46,47]. Extensions to other systems merit future studies.

The authors thank M. Ezawa and K. Kikutake for fruitful discussions. This work was supported by JSPS Grant-in-Aid for Scientific Research (Grants No. 24224009, No. 26103006, No. 26287088, No. 15H05855, No. 16H06717, and No. JP16J02240), from MEXT, Japan, and the ImPACT Program of the Council for Science, Technology and Innovation (Cabinet office, Government of Japan).

Note added.—Recently, a preprint on a closely related topic was released [48].

[1] M. V. Berry, Proc. R. Soc. A **392**, 45 (1984).
[2] G. Herzberg and H. C. Longuet-Higgins, Discuss. Faraday Soc. **35**, 77 (1963).
[3] H. C. Longuet-Higgins, Proc. R. Soc. A **344**, 147 (1975).
[4] J. J. Sakurai, *Modern Quantum Mechanics* (Addison-Wesley, Reading, MA, 1993).
[5] K. Ohgushi, S. Murakami, and N. Nagaosa, Phys. Rev. B **62**, R6065 (2000).
[6] Y. Taguchi, Y. Oohara, H. Yoshizawa, N. Nagaosa, and Y. Tokura, Science **291**, 2573 (2001).
[7] D. J. Thouless, M. Kohmoto, M. P. Nightingale, and M. den Nijs, Phys. Rev. Lett. **49**, 405 (1982).
[8] C. L. Kane and E. J. Mele, Phys. Rev. Lett. **95**, 146802 (2005).
[9] G. Sundaram and Q. Niu, Phys. Rev. B **59**, 14915 (1999).
[10] J. E. Moore and J. Orenstein, Phys. Rev. Lett. **105**, 026805 (2010).
[11] I. Sodemann and L. Fu, Phys. Rev. Lett. **115**, 216806 (2015).
[12] D. J. Thouless, Phys. Rev. B **27**, 6083 (1983).
[13] Q. Niu and D. J. Thouless, J. Phys. A **17**, 2453 (1984).
[14] For a review, see: D. Xiao, M. C. Chang, and Q. Niu, Rev. Mod. Phys. **82**, 1959 (2010).
[15] For a review, see: V. M. Fridkin, Crystallogr. Rep. (Transl. Kristallografiya) **46**, 654 (2001).
[16] S. Ebihara, K. Fukushima, and T. Oka, Phys. Rev. B **93**, 155107 (2016).
[17] K. Taguchi, T. Imaeda, M. Sato, and Y. Tanaka, Phys. Rev. B **93**, 201202 (2016).
[18] S. Murakami, New J. Phys. **9**, 356 (2007).
[19] X. Wan, A. M. Turner, A. Vishwanath, and S. Y. Savrasov, Phys. Rev. B **83**, 205101 (2011).
[20] A. A. Burkov and L. Balents, Phys. Rev. Lett. **107**, 127205 (2011).
[21] G. Xu, H. Weng, Z. Wang, X. Dai, and Z. Fang, Phys. Rev. Lett. **107**, 186806 (2011).
[22] C. Fang, M. J. Gilbert, X. Dai, and B. A. Bernevig, Phys. Rev. Lett. **108**, 266802 (2012).
[23] Y. Chen, D. L. Bergman, and A. A. Burkov, Phys. Rev. B **88**, 125110 (2013).
[24] Y. Yamaji and M. Imada, Phys. Rev. X **4**, 021035 (2014).
[25] T. Guan, C. Lin, C. Yang, Y. Shi, C. Ren, Y. Li, H. Weng, X. Dai, Z. Fang, S. Yan, and P. Xiong, Phys. Rev. Lett. **115**, 087002 (2015).
[26] K. Ueda, J. Fujioka, B.-J. Yang, J. Shiogai, A. Tsukazaki, S. Nakamura, S. Awaji, N. Nagaosa, and Y. Tokura, Phys. Rev. Lett. **115**, 056402 (2015).
[27] Z. Tian, Y. Kohama, T. Tomita, H. Ishizuka, T. H. Hsieh, J. J. Ishikawa, K. Kindo, L. Balents, and S. Nakatsuji, Nat. Phys. **12**, 134 (2016).
[28] S.-M. Huang, S.-Y. Xu, I. Belopolski, C.-C. Lee, G. Chang, B. Wang, N. Alidoust, M. Neupane, H. Zheng, D. Sanchez, A. Bansil, G. Bian, H. Lin, and M. Zahid Hasan, Proc. Natl. Acad. Sci. U.S.A. **113**, 1180 (2016).
[29] Q. Chen and G. A. Fiete, Phys. Rev. B **93**, 155125 (2016).
[30] S.-M. Huang, S.-Y. Xu, I. Belopolski, C.-C. Lee, G. Chang, B. Wang, N. Alidoust, G. Bian, M. Neupane, C. Zhang, S. Jia, A. Bansil, H. Lin, and M. Zahid Hasan, Nat. Commun. **6**, 7373 (2015).
[31] H. Weng, C. Fang, Z. Fang, B. A. Bernevig, and X. Dai, Phys. Rev. X **5**, 011029 (2015).
[32] B. Q. Lv, H. M. Weng, B. B. Fu, X. P. Wang, H. Miao, J. Ma, P. Richard, X. C. Huang, L. X. Zhao, G. F. Chen, Z. Fang, X. Dai, T. Qian, and H. Ding, Phys. Rev. X **5**, 031013 (2015).
[33] S.-Y. Xu, I. Belopolski, N. Alidoust, M. Neupane, G. Bian, C. Zhang, R. Sankar, G. Chang, Z. Yuan, C. C. Lee, S.-M. Huang, H. Zheng, J. Ma, D. S. Sanchez, B. Wang, A. Bansil, F. Chou, P. P. Shibayev, H. Lin, S. Jia, and M. Zahid Hasan, Science **349**, 613 (2015).
[34] Y. Sun, S.-C. Wu, and B. Yan, Phys. Rev. B **92**, 115428 (2015).
[35] The coupling g is given as $g = \langle n|q_e|\delta r||m\rangle$, where $|m\rangle$ and $|n\rangle$ are Wannier functions; we used $\langle n||\delta r||m\rangle \sim 10^{-10}$ m for the estimation.
[36] The magnitude of $\alpha_{1,2}$ is estimated from an assumption $vb \sim \alpha_{1,2}b^2$, where $b \sim 10^{10}$ m^{-1} is the length of the reciprocal vectors.
[37] H. B. Neilsen and M. Ninomiya, Phys. Lett. B **B105**, 219 (1981); Nucl. Phys. **B185**, 20 (1981); **B193**, 173 (1981).
[38] T. Morimoto and N. Nagaosa, Phys. Rev. Lett. **117**, 146603 (2016).
[39] C.-K. Chan, P. A. Lee, K. S. Burch, J. H. Han, and Y. Ran, Phys. Rev. Lett. **116**, 026805 (2016).
[40] H. B. Nielsen and M. Ninomiya, Phys. Lett. B **130**, 389 (1983).
[41] K. Fukushima, D. E. Kharzeev, and H. J. Warringa, Phys. Rev. D **78**, 074033 (2008).
[42] D. T. Son and B. Z. Spivak, Phys. Rev. B **88**, 104412 (2013).
[43] T. Hayata and M. Ueda, arXiv:1606.03589.
[44] D. Hsieh, D. Qian, L. Wray, Y. Xia, Y. S. Hor, R. J. Cava, and M. Z. Hasan, Nature (London) **452**, 970 (2008).
[45] L. Li, J. G. Checkelsky, Y. S. Hor, C. Uher, A. F. Hebard, R. J. Cava, and N. P. Ong, Science **321**, 547 (2008).
[46] K. Sun, H. Yao, E. Fradkin, and S. A. Kivelson, Phys. Rev. Lett. **103**, 046811 (2009).
[47] W. Witczak-Krempa and Y. B. Kim, Phys. Rev. B **85**, 045124 (2012).
[48] C.-K. Chan, N. H. Linder, G. Rafael, and P. A. Lee, arXiv:1607.07839.